Physics Letters B 744 (2015) 142–145

Contents lists available at ScienceDirect

Physics Letters B

www.elsevier.com/locate/physletb

# Geometrical scaling behavior of the top structure functions ratio at the LHeC

G.R. Boroun

*Physics Department, Razi University, Kermanshah 67149, Iran*

ARTICLE INFO

*Article history:*
Received 11 March 2015
Accepted 23 March 2015
Available online 27 March 2015
Editor: A. Ringwald

*Keywords:*
Charm structure function
Gluon distribution
Hard pomeron
Small-$x$

ABSTRACT

We consider the ratio of the top structure functions $R^t(\tau_t)$ in top pair production as a probe of the top content of the proton at the LHeC project. We study the top structure functions with the geometrical scaling of gluon distribution at small $x$ and show that top reduced cross section exhibits geometrical scaling in a large range of photon vitualities. This analysis shows that top longitudinal structure function has sizeable impact on the top reduced cross section at $Q^2 \approx 4m_t^2$.



Recently, a method of determination of the top structure function in the proton from the LHeC project [1,2] had been proposed [3]. On the basis of the method it is known that the dominant source for the $F_2^t$ scaling violations is the conversion of gluons into the $t\bar{t}$ pairs at low-$x$. The initial scaling increases as $Q^2$ increases from $x_0 = 0.0001$–$0.1$ to $Q^2 = 10$–$10\,000$ GeV$^2$ respectively. In this limit, the crucial point is the observation that the top structure function parameterization depends directly on the gluon density. The relevant framework for the dominance of the gluon distributions in perturbative QCD in this limit is the leading $\log(1/x)$ $(LL1/x)$ approximation. The basic quantity in this approximation is the non-integrated gluon distribution $f(x, k_T^2)$ which is related to the conventional gluon density $g(x, Q^2)$, which satisfies DGLAP evolution, as

$$xg(x, Q^2) = \int_0^{Q^2} \frac{dk_T^2}{k_T^2} f(x, k_T^2). \tag{1}$$

The analytical behavior for $f(x, k_T^2)$ at small $x$ is found to be given by [4], if the running coupling constant effects are taken into account, as

$$f(x, k_T^2) \sim \mathcal{R}(x, k_T^2) x^{-\lambda} \tag{2}$$

where $\lambda = 4\frac{N_c\alpha_s}{\pi}\ln(2)$ at LO and at NLO it has the following form [5]

$$\lambda = 4\frac{N_c\alpha_s}{\pi}\ln(2)[1 - c(\frac{1}{2})\frac{N_c\alpha_s}{4\pi}], \tag{3}$$

and $c(\frac{1}{2}) = 25.8388 + 0.1869\frac{n_f}{N_c} + 10.6584\frac{n_f}{N_c^2}$. The quantity $1 + \lambda$ is equal to the intercept of the so-called BFKL pomeron. The $K_T$-factorization approach relates strongly to Regge-like behavior of gluon distribution, as we restrict our investigations to the gluon distribution function at the following form

$$xg(x, Q^2) \sim x^{-\lambda}. \tag{4}$$

Here $\lambda$ is the hard-pomeron intercept. The credible phenomenology intercept of the BFKL equation can be defined by a kinematic constraint to control the gluon ladder [4]. As the effect of this constraint on the intercept one finds that it reduced the intercept from $\lambda \sim 0.5$ to $\lambda \sim 0.3$ [6]. Recently the value 0.317 was estimated directly from the data in the proton unpolarized structure function [7].

The latest data [8] for charm and beauty structure functions show that there are not enough data for the suggestion of the logarithmic $x$-derivative in the full kinematic range available as [9]

$$\delta = \frac{\partial \ln F_2^{c,b}}{\partial \ln \frac{1}{x}}. \tag{5}$$

For the charm structure functions, the data points at the values $12 \leq Q^2 \leq 120$ GeV$^2$ have shown that this derivative is independent of $x$ for low $x$ values within the experimental data and this

*E-mail addresses:* grboroun@gmail.com, boroun@razi.ac.ir.

http://dx.doi.org/10.1016/j.physletb.2015.03.051

implies that a power law behavior for charm structure function as $<\delta>$ is estimated from fits to the H1 data as $<\delta>\simeq 0.43$. For other $Q^2$ values and the beauty structure functions there are not enough experimental data for this behavior change in the measured kinematic range. Using ideas from Regge theory, where gluon distributions have the same power law behavior (Eq. (4)) for all H1 experimental data for charm and beauty structure functions. Our estimations show that $<\lambda^c>\simeq 0.45\pm^{0.90}_{0.23}$ and $<\lambda^b>\simeq 0.43\pm^{0.21}_{0.33}$ for charm and beauty intercepts respectively. These values for $\lambda$'s show that the hard pomeron behavior [10–13] is dominant. Indeed the hard pomeron behavior gives a very good description of the data within the experimental accuracy, not only for the charm structure function $F_2^c(x,Q^2)$, but also for the beauty structure function $F_2^b(x,Q^2)$.

In leptoproduction, the primary graph is the Photon–Gluon–Fusion (PGF) model where the incident virtual photon interacts with a gluon from the target nucleon for producing $t\bar{t}$ at leading order (LO) and next-leading-order (NLO) processes at the LHeC project [1,2] within the variable-flavor-number scheme (VFNS). In the LHeC project, we think that the top quark component $F_2^t$ of $F_2$ is apparently governed almost entirely by hard-pomeron exchange over a wide range of $x$ and $Q^2$. In LHeC project, for $Q^2>2$ GeV$^2$, the hard pomeron behavior is driven solely by the gluon field. Therefore, according to perturbative QCD, the top quark originates from a gluon structure function that is dominated at small $x$ by hard pomeron exchange.

Let us use the gluon distribution to calculate top production in LO up to NLO pQCD at small $x$ as the top structure functions may be given by

$$F_k^t(x,Q^2,m_t^2)=e_t^2\frac{\alpha_s(<\mu_t^2>)}{2\pi}\int_{1-\frac{1}{a}}^{1-x}dzC_{g,2}^t(1-z,\zeta)\times G(\frac{x}{1-z},<\mu_t^2>),(k=2\,\&\,L) \tag{6}$$

where $C_{g,k}^t$ are the coefficient functions and $a=1+\xi$ where $\xi\equiv\frac{m_t^2}{Q^2}$ and $G\,(=xg)$ is the gluon momentum distribution. The physical intuition leads us to take $<\mu_t^2>=4m_t^2+Q^2/2$ for both, though it must be recognized that this is a mere guess. The value $m_t=157$ GeV is fixed for these results.

Thus, exploiting the hard pomeron behavior (4) for the gluon distribution at $x^{-\lambda}\gg 1$ and using the NLO approximation for collinear coefficient functions and anomalous dimensions of Wilson operators, the top structure functions $F_k^t$, with respect to the gluon distribution behavior, have the following forms

$$F_k^t(x,Q^2,m_t^2)=e_t^2\frac{\alpha_s(<\mu^2>)}{2\pi}\eta_k(x,<\mu^2>)\times G(x,<\mu^2>), \tag{7}$$

where

$$\eta_k(x,<\mu^2>)=C_{g,k}^t(x,\zeta)\otimes(x)^\lambda, \tag{8}$$

and the symbol $\otimes$ denotes convolution according to the usual prescription, $f(x)\otimes g(x)=\int_x^1(dy/y)f(y)g(x/y)$. The ratios of the top structure functions are important for investigation of the photon-top quark scattering contribution to the Callan–Gross ratio at low and moderate $Q^2\simeq m_t^2$ as

$$R^t(x,Q^2)=\frac{F_L^t(x,Q^2)}{F_2^t(x,Q^2)}. \tag{9}$$

The solution of Eq. (9) is straightforward and given by

$$R^t(x,Q^2)=\frac{e_t^2\frac{\alpha_s(<\mu^2>)}{2\pi}\eta_L(x,<\mu^2>)G(x,<\mu^2>)}{e_t^2\frac{\alpha_s(<\mu^2>)}{2\pi}\eta_2(x,<\mu^2>)G(x,<\mu^2>)}=\frac{\eta_L(x,<\mu^2>)}{\eta_2(x,<\mu^2>)}.$$

In general, we write the quantity $R^t$ by the following form

$$R^t(x,Q^2)=\frac{C_{g,L}^t(x,\zeta)\otimes(x)^\lambda}{C_{g,2}^t(x,\zeta)\otimes(x)^\lambda}. \tag{10}$$

In fact, the gluon distribution input cancels in the ratio. Therefore the reduced cross section for photon-top quark production [14] is given by

$$\tilde{\sigma}^{t\bar{t}}(x,Q^2)=F_2^t(x,Q^2)[1-\frac{y^2}{1+(1-y)^2}\frac{\eta_L(x,<\mu^2>)}{\eta_2(x,<\mu^2>)}], \tag{11}$$

where $y\,(=\frac{Q^2}{sx})$ is the inelasticity variable and $s$ is the square of the center-of-mass energy of the virtual photon-top quark subprocess $Q^2(1-z)/z$. H1 Collab. [8] obtained the charm and beauty structure functions $F_2^{c\bar{c}}$ and $F_2^{b\bar{b}}$ from the measured $c$ and $b$ cross sections after applying small corrections for the longitudinal structure functions $F_L^{c\bar{c}}$ and $F_L^{b\bar{b}}$ at low and moderate inelasticity. The inelasticity values for $c$ and $b$ production in this experiment were in the region $0.09<y<0.5$. We expect the inelasticity value for $t$ production to be at high values. The high $y$ values at the top production are according to the very low $x$ values, as in this region the screening (or shadowing) effects are very important. The main effect of shadowing is the recombining of gluons at higher densities via the process $gg\to g$, where it causes the top structure behavior to be tamed. The saturation limit for the gluon distribution is at the order of the hadronic radius $R_H$ as $G_{sat}(x,Q^2)\sim R_H^2Q^2/\alpha_s(Q^2)$. Because the gluons are concentrated around the hot-spot points, where the radius $R_{hs}$ is smaller than the hadronic radius $R_H$, the linear effects must be modified by the nonlinear terms as have been formalized by GLRMQ [15].

However at low-$y$, where $F_L^t$ is set to zero we have $\tilde{\sigma}^{t\bar{t}}(x,Q^2)$ $(\equiv\tilde{\sigma}^{t\bar{t}}_{F_2})=F_2^t(x,Q^2)$. But at moderate and high inelasticity, the longitudinal structure function contributes to the cross section. The fractional $F_L^t$ contribution to the top cross section is investigated by

$$C_{F_L^t}\equiv|\frac{\tilde{\sigma}^{t\bar{t}}-\tilde{\sigma}^{t\bar{t}}_{F_2}}{\tilde{\sigma}^{t\bar{t}}}|. \tag{12}$$

Indeed, there is a sizeable contribution to the top cross section at the LHeC project at high $y$ and very low $x$ values. The LHeC can use a proton beam with energy up to 7 TeV, and the electron beam energy is set to 60 GeV. At fixed $(x,y)$, the gain in $\sqrt{s}$ will be a factor of about 4 as compared to HERA. The kinematic range of the LHeC for determination of the top structure function is at low $x$ and at high $Q^2$ [16,17]. At small $x$, the inelasticity is given as $y\simeq 1-E'_e/E_e$. Therefore, we can choose the extremum value for the inelasticity as if $y\to 1$, then $f(y)=y^2/Y_+\to 1$ where $Y_+=1+(1-y)^2$.

Therefore, the $t\bar{t}$-pair production at the LHeC project in DIS can happen at small enough $x$ where the geometrical scaling (SC) has been introduced [18] in this region as the dense gluon system is fully justified. Thus the saturation scale $Q_s^2(x)$, is an intrinsic characteristic this dense gluon system which tame the rise of the gluon distribution at small $x$. One thus finds that the saturation scale has the form $Q_s^2(x)=Q_0^2(x/x_0)^{-\lambda}$ as it increases with decreasing $x$. This type of scaling is also found to be an intrinsic property of the

**Table 1**
The fractional $F_L^t$ contribution to the top reduced cross section in bins for top production at the LHeC.

| $Q^2$ (GeV$^2$) | $C_{F_L^t}$ |
|---|---|
| 10 | 0.27E-4 |
| 100 | 0.27E-3 |
| 1000 | 0.27E-2 |
| 10 000 | 0.025 |
| 100 000 | 0.150 |
| 1 000 000 | 0.253 |
| 10 000 000 | 0.200 |
| 100 000 000 | 0.146 |
| 1 000 000 000 | 0.113 |
| 10 000 000 000 | 0.092 |

nonlinear evolution equations. Therefore the proton cross section depends upon the single variable $\tau = Q^2/Q_s^2(x)$, as

$$\sigma_{\gamma^* p}(x, Q^2) = \sigma_{\gamma^* p}(\tau). \tag{13}$$

The gluon distribution at the geometric scale is defined by

$$\frac{\alpha_s}{2\pi} xg(x, Q^2 = Q_s^2(x)) = r_0 x^{-\lambda}, \tag{14}$$

with $r_0 = \frac{3}{8\pi^3}\sigma_0 x_0^{\lambda}$. The two parameters $\sigma_0$ and $x_0$ determined when the authors in Ref. [19] performed a fit including charm to the total cross section $\sigma^{\gamma^* p}$. Using the leading-twist relationship between the dipole cross section and the unintegrated gluon distribution, the integrated gluon distribution at fixed coupling is given by [20]

$$G(x, Q^2) = \frac{3\sigma_0}{4\pi^2\alpha_s}(-Q^2 e^{-Q^2(\frac{x}{x_0})^{\lambda}} + (\frac{x_0}{x})^{\lambda}(1 - e^{-Q^2(\frac{x}{x_0})^{\lambda}})). \tag{15}$$

Therefore we use the same parameters as those found from a fit to small $x$ data [19]. But $Q_0^2$ have to be larger than 2 GeV$^2$ and the Bjorken variable $x = x_B$ was modified [21] to be

$$x = x_B(1 + \frac{4m_t^2}{Q^2}). \tag{16}$$

In top production the geometrical scaling violation is expected due to the large top quark mass, therefore we use the scaling variable $\tau_t$ according to the top quark mass further than the historical variable [22] as

$$\tau_t = (1 + \frac{4m_t^2}{Q^2})^{1+\lambda}\frac{Q^2}{Q_0^2}(\frac{x_B}{x_0})^{\lambda}. \tag{17}$$

This new scale is valid in the small $x$ as top pair production is dominant in this region. Therefore the saturation model leads to

$$F_k^t(\tau_t) = e_t^2(\frac{3\sigma_0}{8\pi^3}(-\mu^2 e^{-\mu^2(\frac{x}{x_0})^{\lambda}} + (\frac{x_0}{x})^{\lambda}(1 - e^{-\mu^2(\frac{x}{x_0})^{\lambda}})))\eta_k(\tau_t). \tag{18}$$

Finally the reduced cross section for top pair production in DIS at the LHeC project is bounded by the geometrical scaling which assures unitarity of $F_2^t$ at the limit $y \to 1$, as

$$\widetilde{\sigma}^{t\bar{t}}(\tau_t) \to F_2^t(\tau_t)[1 - R^t(\tau_t)]. \tag{19}$$

In Table 1, we find a sizable contribution to the reduced cross section at high $y$. This overlaps with the high $Q^2$ and very low $x$ region which is outside the kinematic region accessed at LHeC as $0.000002 < x < 0.8$ and $2 < Q^2 < 100\,000$ GeV$^2$. We see

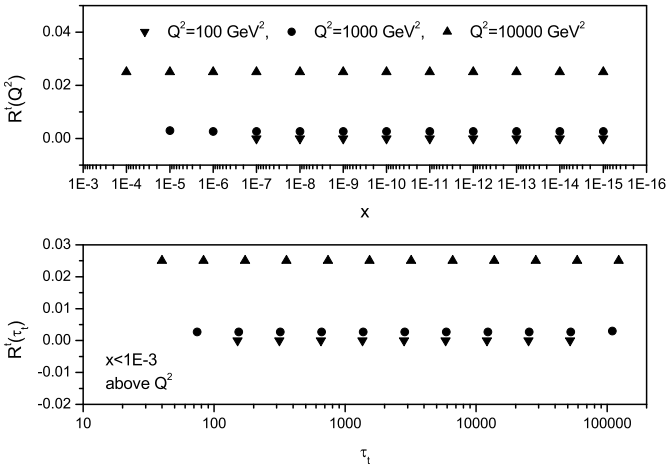


**Fig. 1.** The ratio $R^t$ as a function of $x$ and $\tau_t$ for different values of $Q^2$.

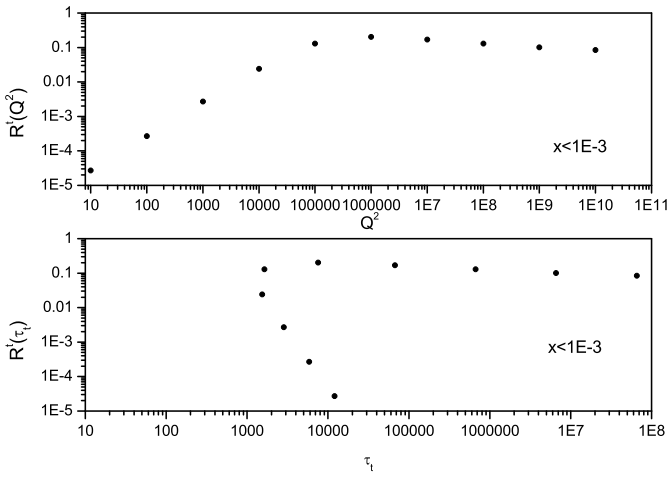


**Fig. 2.** The ratio $R^t$ as a function of $Q^2$ and $\tau_t$ with $<\mu^2> = 4m_t^2 + Q^2/2$.

that the corresponding longitudinal top structure function is almost zero for $Q^2 \leq 1000$ GeV$^2$ at very low $x$ values. In this case, $\widetilde{\sigma}^{t\bar{t}}(\tau_t) = F_2^t(\tau_t)$. In Figs. 1 and 2, we show the ratio $R^t$ in this limit. This value is non-zero for $Q^2 > 1000$ GeV$^2$ and has a maximum value less than 0.21 practically at $Q^2 \simeq 1E6$. Our results show that the ratio $R^t$ is independent of the $x$ values and it has the same behavior for the charm and beauty production [23–27] in the entire region of $Q^2$. We conclude that the longitudinal top structure function component of the reduced cross section could be a good probe of the top density of the proton at $Q^2 \simeq 4m_t^2$.

One can also see from Figs. 1 and 2 the behavior of the top structure functions ratio versus the top scaling variable $\tau_t$ for different values of $Q^2$. In Fig. 3 we show the top structure functions with $x < 1E-3$ for different values of $Q^2$ against the scaling variable $\tau_t$. We see that the results exhibit geometrical scaling over a very broad range of $Q^2$ at any $Q^2$ scale. We can also clearly see (in Figs. 3 and 4) that the behavior of the $\widetilde{\sigma}^{t\bar{t}}(\tau_t)$ and $F_2^t(\tau_t)$ on $\tau_t$ is approximately $1/\tau_t$ at large $\tau_t$. The transition point is placed at $\tau \simeq 0.45$ which has value much less than $\mu_t^2 = 4m_t^2$ for a top mass $m_t = 157$ GeV. At this point the $Q_s^2$ has value of order 200 000 GeV$^2$, where in this region $Q^2 << Q_s^2$ and the nonlinear effects are important as the gluon density grows by the rate $Q_s^2/\Lambda^2$. As plotted in Fig. 5, this transition point will be determined at LHeC project.

In conclusion, we predict the top structure functions at the LHeC domain with respect to the geometrical scaling. We demon-

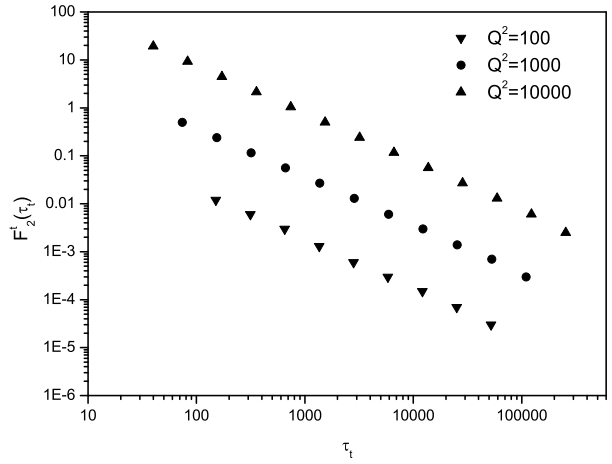


**Fig. 3.** The $F_2^t$ structure function for $Q^2 < 4m_t^2$.

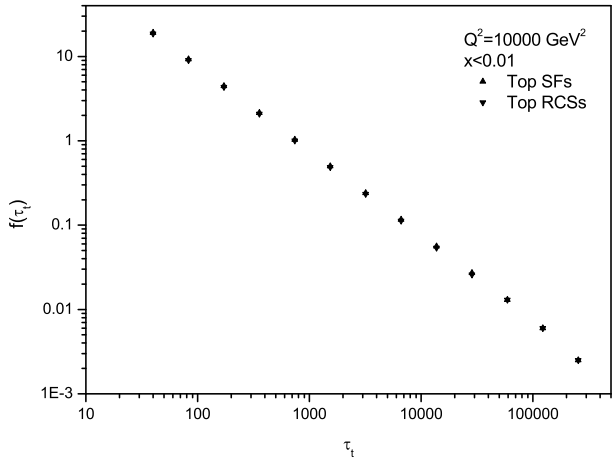


**Fig. 4.** $\widetilde{\sigma}^{t\bar{t}}$ (top RCSs) and $F_2^t$ (top SFs) plotted versus the top scaling variable $\tau_t$.

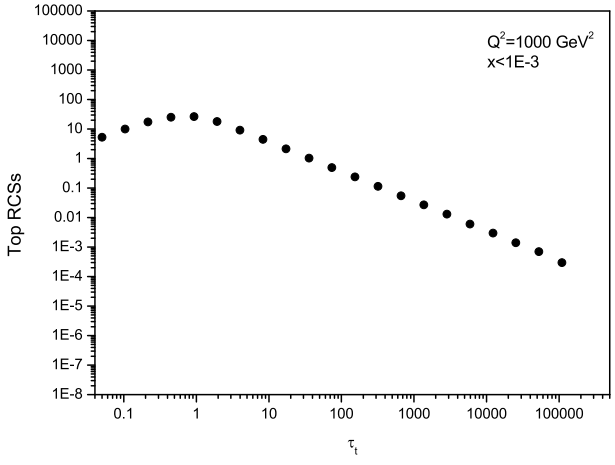


**Fig. 5.** The top reduced cross section $\widetilde{\sigma}^{t\bar{t}}$ from the region $x < 0.001$ plotted versus the top scaling variable $\tau_t$.

strated the usefulness of the direct extraction $F_2^t$ from the top reduced cross section $\widetilde{\sigma}^{t\bar{t}}$ as the top longitudinal structure function has a correlation function at $Q^2 \geq 4m_t^2$. Also we show the ratio of the top structure functions as it is independent of $x$ at low $x$ values and it has the same behavior as considered for charm and beauty structure function ratios. The maximum value estimated for $R^t(\tau_t)$ is almost $\sim$0.2 in a wide region of $x$. The most important numerical sources of theoretical uncertainty in $t\bar{t}$-pair production are the factorization scale dependence and the constant parameters in the saturation model. Finally we show the geometrical scaling in the top structure functions from the region $x < 0.01$ and a transition in the behavior on $\tau_t$.

## Acknowledgements

The author is grateful to Prof. B. Kniehl and Prof. N. Armesto for their suggestions, to Prof. A. Kotikov for reading the manuscript and to Prof. N.Ya. Ivanov for reading and useful comments.

## References

[1] P. Newman, Nucl. Phys., Proc. Suppl. 191 (2009) 307;
S.J. Brodsky, arXiv:1106.5820 [hep-ph], 2011;
Amanda Cooper-Sarkar, arXiv:1310.0662 [hep-ph], 2013.
[2] LHeC Study group, CERN-OPEN-2012-015;
F.D. Aaron, et al., H1 and ZEUS Collaboration, J. High Energy Phys. 1001 (2010) 109, arXiv:0911.0884 [hep-ex];
LHeC Study group, LHeC-Note-2012-005 GEN.
[3] G.R. Boroun, arXiv:1411.6492 [hep-ph], Phys. Lett. B 741 (2015) 197.
[4] J. Kwiecinski, J. Phys. G 19 (1993) 1443;
J. Kwiecinski, A.D. Martin, R. Roberts, W.J. Stirling, Phys. Rev. D 42 (1990) 3645.
[5] V.S. Fadin, L.N. Lipatov, Phys. Lett. B 429 (1998) 127.
[6] A.M. Cooper-Sarkar, R.C.E. Devenish, Acta Phys. Pol. B 34 (2003) 2911.
[7] A.A. Godizov, Nucl. Phys. A 927 (2014) 36.
[8] F.D. Aaron, et al., H1 Collaboration, Eur. Phys. J. C 65 (2010) 89.
[9] A. Kotikov, arXiv:1212.3733 [hep-ph], 2012.
[10] A. Donnachie, P.V. Landshoff, Phys. Lett. B 296 (1992) 257;
A. Donnachie, P.V. Landshoff, Phys. Lett. B 437 (1998) 408.
[11] A. Donnachie, P.V. Landshoff, Phys. Lett. B 550 (2002) 160;
A. Donnachie, P.V. Landshoff, Phys. Lett. B 533 (2002) 277;
A. Donnachie, P.V. Landshoff, Phys. Lett. B 595 (2004) 393.
[12] P.V. Landshoff, arXiv:hep-ph/0203084.
[13] J.R. Cudell, G. Soyez, Phys. Lett. B 516 (2001) 77;
J.R. Cudell, A. Donnachie, P.V. Landshoff, Phys. Lett. B 448 (1999) 281.
[14] A.Y. Illarionov, B.A. Kniehl, A.V. Kotikov, Phys. Lett. B 663 (2008) 66;
A.Y. Illarionov, A.V. Kotikov, Phys. At. Nucl. 75 (2012) 1234.
[15] A.H. Mueller, J. Qiu, Nucl. Phys. B 268 (1986) 427;
L.V. Gribov, E.M. Levin, M.G. Ryskin, Phys. Rep. 100 (1983) 1.
[16] Workshop on the LHeC, 20–21 January 2014, Chavannes-de-Bogis, Switzerland, http://cern.ch/lhec.
[17] J.L. Abelleira Fernandez, et al., LHeC group, arXiv:1206.2913v1 [physics.acc-ph], 13 June 2012.
[18] A.M. Stasto, K.J. Golec-Biernat, J. Kwiecinski, Phys. Rev. Lett. 86 (596) (2001).
[19] K. Golec-Biernat, M. Wusthoff, Phys. Rev. D 59 (1998) 014017.
[20] R.S. Thorne, Phys. Rev. D 71 (2005) 054024.
[21] G. Beuf, C. Royon, D. Salek, arXiv:0810.5082 [hep-ph].
[22] T. Stebel, arXiv:1305.2583 [hep-ph].
[23] N.N. Nikolaev, V.R. Zoller, Phys. At. Nucl. 73 (2010) 672;
N.N. Nikolaev, V.R. Zoller, Phys. Lett. B 509 (2001) 283;
N.N. Nikolaev, J. Speth, V.R. Zoller, Phys. Lett. B 473 (2000) 157;
R. Fiore, N.N. Nikolaev, V.R. Zoller, JETP Lett. 90 (2009) 319.
[24] A.V. Kotikov, A.V. Lipatov, G. Parente, N.P. Zotov, Eur. Phys. J. C 26 (2002) 51.
[25] N.Ya. Ivanov, B.A. Kniehl, Eur. Phys. J. C 59 (2009) 647;
N.Ya. Ivanov, Nucl. Phys. B 814 (2009) 142;
N.Ya. Ivanov, Eur. Phys. J. C 59 (2009) 647.
[26] I.P. Ivanov, N. Nikolaev, Phys. Rev. D 65 (2002) 054004.
[27] N.N. Nikolaev, V.R. Zoller, Phys. Lett. B 509 (2001) 283;
N.N. Nikolaev, V.R. Zoller, Phys. At. Nucl. 73 (2010) 672;
V.R. Zoller, Phys. Lett. B 509 (2001) 69.